

Journal Pre-proof

Immunotoxic mechanisms of cigarette smoke and heat-not-burn tobacco vapor on Jurkat T cell functions

Pablo Scharf, Gustavo H.O. da Rocha, Silvana Sandri, Cintia S. Heluany, Walter R. Pedreira Filho, Sandra H.P. Farsky



PII: S0269-7491(20)36552-0

DOI: <https://doi.org/10.1016/j.envpol.2020.115863>

Reference: ENPO 115863

To appear in: *Environmental Pollution*

Received Date: 30 June 2020

Revised Date: 29 September 2020

Accepted Date: 14 October 2020

Please cite this article as: Scharf, P., da Rocha, G.H.O., Sandri, S., Heluany, C.S., Pedreira Filho, W.R., Farsky, S.H.P., Immunotoxic mechanisms of cigarette smoke and heat-not-burn tobacco vapor on Jurkat T cell functions, *Environmental Pollution*, <https://doi.org/10.1016/j.envpol.2020.115863>.

This is a PDF file of an article that has undergone enhancements after acceptance, such as the addition of a cover page and metadata, and formatting for readability, but it is not yet the definitive version of record. This version will undergo additional copyediting, typesetting and review before it is published in its final form, but we are providing this version to give early visibility of the article. Please note that, during the production process, errors may be discovered which could affect the content, and all legal disclaimers that apply to the journal pertain.

© 2020 Elsevier Ltd. All rights reserved.

Author Statement

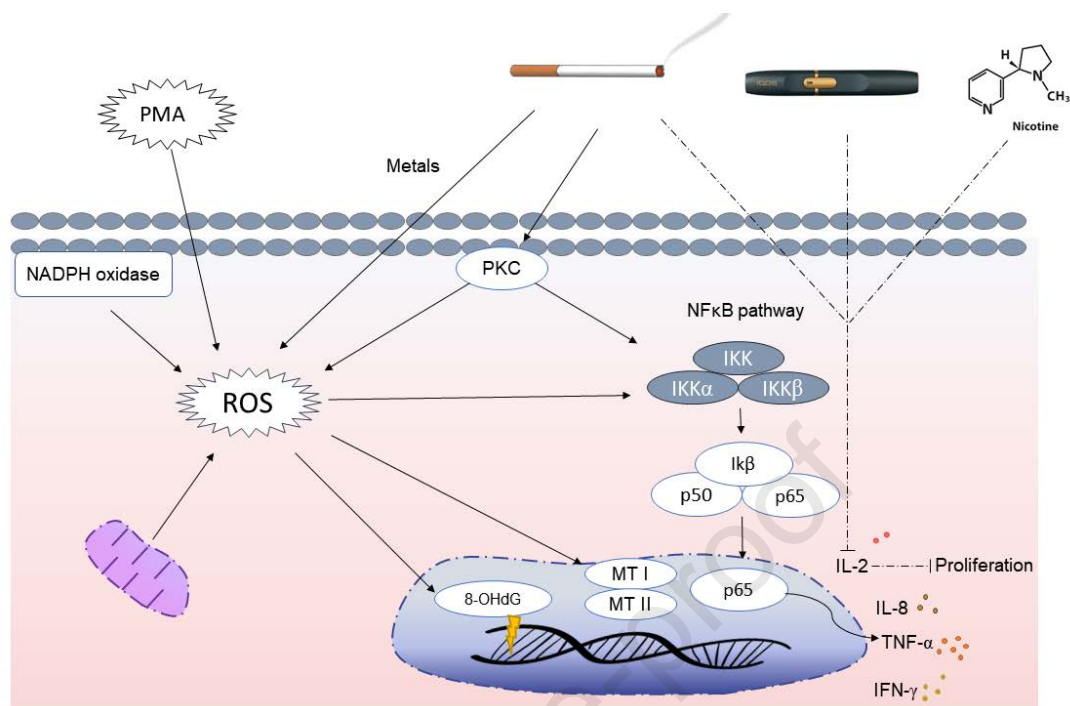
Manuscript: Immunotoxic mechanisms of cigarette smoke and heat-not-burn tobacco vapor on Jurkat T cell functions

All authors listed in this scientific research contributed to its elaboration. The authorship contributions are listed below:

- **Conception and design of study:** Pablo Scharf and Sandra H. P. Farsky.
- **Data acquisition:** Pablo Scharf, Gustavo Henrique Oliveira da Rocha, Silvana Sandri, Cintia Heluany, Walter R. Pedreira Filho
- **Data analysis:** Pablo Scharf, Gustavo Henrique Oliveira da Rocha, Silvana Sandri, Cintia Heluany, Walter R. Pedreira Filho
- **Drafting the manuscript:** Pablo Scharf and Sandra H. P. Farsky
- **Manuscript Revising:** Pablo Scharf, Gustavo Henrique Oliveira da Rocha and Sandra H. P. Farsky

All authors approved the final version of the manuscript to be published

Pablo Scharf, Gustavo Henrique Oliveira da Rocha, Silvana Sandri, Cintia Heluany, Walter R. Pedreira Filho and Sandra Farsky



**Immunotoxic mechanisms of cigarette smoke and heat-not-burn tobacco vapor
on Jurkat T cell functions**

Pablo Scharf¹; Gustavo H. O. da Rocha¹; Silvana Sandri¹; Cintia S. Heluany¹; Walter
R. Pedreira Filho²; Sandra H. P. Farsky^{1*}

¹Department of Clinical & Toxicological Analyses, School of Pharmaceutical
Sciences, University of Sao Paulo, SP, Brazil

²Fundação Jorge Duprat Figueiredo de Segurança e Medicina do Trabalho, Ministério
do Trabalho e Previdência Social, Sao Paulo, SP, Brazil

*Correspondence to Sandra H. P. Farsky, Department of Clinical & Toxicological
Analyses, School of Pharmaceutical Sciences, University of Sao Paulo, Brazil. E-
mail: sfarsky@usp.br

Abstract

Cigarette smoke (CS) affects immune functions, leading to severe outcomes in smokers. Robust evidence addresses the immunotoxic effects of combustible tobacco products. As heat-not-burn tobacco products (HNBT) vaporize lower levels of combustible products, we here compared the effects of cigarette smoke (CS) and HNBT vapor on Jurkat T cells. Cells were exposed to air, conventional cigarettes or heatsticks of HNBT for 30 minutes and were stimulated or not with phorbol myristate acetate (PMA). Cell viability, proliferation, reactive oxygen species (ROS) production, 8-OHdG, MAP-kinases and nuclear factor κ B (NF κ B) activation and metallothionein expression (MTs) were assessed by flow cytometry; nitric oxide (NO) and cytokine levels were measured by Griess reaction and ELISA, respectively. Levels of metals in the exposure chambers were quantified by inductively coupled plasma mass spectrometry. MT expressions were quantified by immunohistochemistry in the lungs and liver of C57Bl/6 mice exposed to CS, HNBT or air (1 hour, twice a day for five days: via inhalation). While both CS and HNBT exposures increased cell death, CS led to a higher number of necrotic cells, increased the production of ROS, NO, inflammatory cytokines and MTs when compared to HNBT-exposed cells, and led to a higher expression of MTs in mice. CS released higher amounts of metals. CS and HNBT exposures decreased PMA-induced interleukin-2 (IL-2) secretion and impaired Jurkat proliferation, effects also seen in cells exposed to nicotine. Although HNBT vapor does not activate T cells as CS does, exposure to both HNBT and CS suppressed proliferation and IL-2 release, a pivotal cytokine involved with T cell proliferation and tolerance, and this effect may be related to nicotine content in both products.

Key words: T cell proliferation; metallothionein; Jurkat cells; Interleukin-2; nicotine; metals

75 Main findings:

76 CS exposure displayed more severe toxic effects in Jurkat T cells than HNBT vapor; nevertheless, such
77 CS and HNBT impaired IL-2 secretion and cell proliferation, which may be due to nicotine actions.

Journal Pre-proof

INTRODUCTION

Smoking is a global public health challenge and considered the leading cause of preventable death in the world. Tobacco, during combustion, releases almost 8,700 chemical compounds, including 69 known carcinogens (IARC 2014; Stabbert et al. 2017). Exposures to first or secondhand cigarette smoke are related to development and aggravation of respiratory (Warren and Cummings 2013) and cardiovascular diseases (Mainali et al. 2014), carcinogenesis (Hecht 2012), type II diabetes (Sliwinska-Mossori, 2017) and auto-immune diseases (Qiu et al. 2016).

Smoking is known to affect both innate and adaptive immunity (Gonçalves et al. 2011). Tobacco exposure leads to exacerbation or impairment of activation of immune pathways and is considered an environmental risk factor for the development and worsening of severe diseases, such as chronic obstructive pulmonary disease (Koch et al. 2006), rheumatoid arthritis (Nguyen et al. 2013), Chron's disease (Rubin and Hanauer 2000), diabetes (Sliwinska-Mossori, 2017) and encephalomyelitis (Alrouji et al. 2019). The activation of the aryl hydrocarbon receptor (AhR) in T cells by combustible products of tobacco is described as a major factor in the activation of the immune system and is responsible for the development of autoimmune diseases, especially rheumatoid arthritis (Nguyen et al; 2013; Heluany et al. 2018). Binding of these compounds to AhR favors polarization of pathogenic Th17 cells, with consequent decline of T regulatory cell (Treg) populations (Nguyen et al; 2013; Talbott et al. 2018). Moreover, the generation of reactive oxygen species (ROS) is a hallmark of cytotoxicity generated by several compounds, such as benzene and its metabolites and metals from cigarette smoke combustion (Valavanidis et al. 2009). ROS act as secondary messengers, regulating cell function through redox-activatable signaling systems (Weyand and Goronzy 2018). In T cells, ROS signaling induces Th1 and Th17 subset proliferation and cytokine production, being a potential effector in autoimmune diseases (Abimannan et al. 2016).

Recognizing the damaging effects of conventional cigarettes and tobacco combustion, the industry of tobacco has developed new forms of nicotine delivery. Non-combustible cigarette devices have emerged as promising tools for harm reduction compared to conventional cigarettes, such as electronic cigarettes and heat-not-burn tobacco products (HNBT) (St.Helen et al. 2018). HNBT devices heat tobacco but do not burn it, thus reducing the release of products from its combustion and releasing mainly nicotine, propylene glycol and glycerin (Forster 2018). HNBT producers claim the emission of toxic products is reduced by about 95% (Bentley et al. 2020), which could be the reason for the reduced toxicity. Nevertheless, independent data on the characterization of compounds released by HNBT vapors and their toxic effects are still scarce, considering that nicotine, besides being responsible for addiction in smokers, induces toxic effects.

Nicotine is a sympathomimetic agent which induces the release of catecholamines from neurons and adrenal glands. Nicotine toxic effects on the cardiovascular/renal system have been fully shown, as it hampers heart functions and increases blood pressure, promoting atherosclerosis (Benowitz et al., 1997; 2010; Suzuki et al., 2020; Neunteufl et al., 2002). Nicotine also induces premature senescence of pancreatic beta cell, a hallmark adverse effect of insulin resistance and diabetes genesis (Sun et al., 2020). In the immune system, nicotine impairs the innate response to infectious agents by affecting the response of lung epithelial cells and innate immune cells (Nguyen et

al. 2020). Conversely, by binding to the receptor, nicotine acts as an anti-inflammatory agent, favoring the polarization and proliferation of Treg cells (Wang et al. 2010). Therefore, the role of nicotine on the genesis of diseases evoked by modifications of the immune system caused by CS exposure needs further evaluation.

Considering the above described and that most cytotoxic effects observed in independent studies on HNBT focus mainly on direct effects of vapors on different respiratory cell lines (Leigh et al. 2018; Sohal et al. 2019), we here compared the effects caused by exposure to HNBT vapor to those caused by CS on oxidative balance and inflammatory parameters of T lymphocytes using Jurkat T cells.

MATERIALS AND METHODS

Cell culture and *in vitro* exposures

Jurkat T cell line (clone E6.1) was obtained from Banco de Células do Rio de Janeiro (Rio de Janeiro, RJ, Brazil) and cultured in Roswell Park Memorial Institute (RPMI) 1640 culture medium containing 10 % fetal bovine serum (FBS; GIBCO Invitrogen, Carlsbad, CA) and 1% antibiotics (100 units/mL penicillin, 100 µg/mL streptomycin; GIBCO Invitrogen, Carlsbad, CA) under standard culture conditions in a humidified incubator at 37 °C with 5 % CO₂. Prior to exposure, cells were placed on 12 mm transwell inserts (0.4 µm porosity; Corning, New York, NY, USA) at a density of 1x10⁶ cells/per well and exposed to airflow, 4 conventional cigarettes (Marlboro Red, Philip Morris) or to 5/6 heatsticks of the HNBT device named IQOS (I quit ordinary smoking; Philip Morris International) in an acrylic exposure chamber. Cells suspended in a small volume of culture medium in this manner were exposed to air, HNBT vapor or CS, which occurred through direct contact with the cell suspensions. The exposure system developed (Bonther, Ribeiro Preto, SP, Brazil) consists of two peristaltic pumps, one responsible for pumping airflow, smoke or vapor to the exposure chamber, and another to maintain the continuous flow of culture medium. The exposure protocol consisted of a 2-second cycle of exposure to CS or HNBT vapor (at 45 rpm) followed by 58 seconds of airflow (at 25 rpm), for 30 minutes (Suppl. figure. 1). Continuous flow of serum-free culture medium was maintained at 20 rpm. After the end of exposures, cells were stimulated with 5 nM of phorbol 12-myristate 13-acetate (PMA) to assess the effects of CS or HNBT exposure in an inflammatory context. To analyze the effect of nicotine on cell proliferation and IL-2 secretion, cells were treated with an equivalent concentration of nicotine for 30 minutes (4.25mg/mL; Sigma Aldrich, USA). This concentration is equivalent to the amount of nicotine delivered by CS and by HNBT vapor, which is similar for both (Mallock et al. 2018).

Cell viability and death

Jurkat cells were exposed to air, CS or HNBT vapor and subsequently incubated for 24 hours with vehicle (sterile phosphate-buffered saline; PBS) or PMA (5 nM). Next, cells were washed twice with PBS, and viability was assessed using annexin V conjugated with fluorescein isothiocyanate diluted in a binding buffer (AnxV-FITC, 1:50; BD Biosciences, CA, USA) and propidium iodide (PI; BD Biosciences, CA, USA) double staining. Thirty minutes after AnxV-FICT incubation in the dark at room temperature, 0.5µL of PI diluted in a binding buffer was added to cell suspensions and 10,000 events were acquired by flow cytometry (Accuri C6; Becton Dickinson, USA). The percentage of viable, apoptotic (either early or late apoptosis) and necrotic cells was assessed.

T cell proliferation assay

To monitor the impact of exposures on cell proliferation, Jurkat cells were stained with 5µM carboxyfluorescein succinimidyl ester (CFSE; Thermo Fischer, Carlsbad, CA, USA) for 20 minutes at 37°C, washed once with PBS and resuspended in RPMI 1640 medium containing 10 % FBS. Next, cells were exposed according to the exposure protocol, plated at 5x10⁵/well on a round-bottom 96-well plate (Corning, NY, USA) stimulated with PMA and cultured for 72 hours. In order to investigate the

effects of CS smoke, HNBT vapor and nicotine on cell proliferation, Jurkat T cells were either exposed to CS or HNBT vapor or treated with different concentrations of nicotine (1 μ M, 10 μ M or 100 μ M; Sigma Aldrich, St. Louis, MO, USA) and stimulated with 10IU/mL of recombinant human interleukin-2 (rhIL-2, BD Bioscience, Becton Dickinson, USA). The fluorescence intensity of CFSE-labeled cells was measured by flow cytometry (Accuri C6, Becton Dickinson, USA), and 30.000 events were considered for analyses. Data were represented as MFI fold change in relation to the respective control for each group.

Detection of reactive oxygen species by DCFH-DA assay

The production of reactive oxygen species (ROS) was quantified 45 minutes after the end of exposures in cells stimulated or not by PMA (5 nM; 45 minutes). After incubation (37°C with 5% CO₂), cells were washed once with PBS and incubated with 200 μ L of an 1 mM solution of dichlorofluorescein diacetate (DCFH-DA; Invitrogen, Carlsbad, CA, USA) for 30 minutes in the dark (37°C with 5% CO₂). Thereafter, 200 μ L of cold PBS were added and 10,000 events were recorded by flow cytometry (Accuri C6; Becton Dickinson, USA). Data were presented as median fluorescence intensity (MFI).

Quantification of nitric oxide by Griess assay

Jurkat cells were exposed to air, CS or HNBT vapor and subsequently incubated for 24 hours with vehicle or PMA (5 nM) and the supernatants were collected to quantify nitric oxide using Griess reaction. Briefly, 100 μ L of supernatant were added to 100 μ L of Griess reagent (solution of 1% sulfanilamide and 0.1% alpha-naphthyl ethylenediamine - Sigma Aldrich, St Louis, MO, USA). After 10 minutes of incubation at room temperature, absorbance was determined by spectrophotometry (Spectra Max 190, Molecular Devices, Sunnyvale, CA, USA) at 550nm wavelength.

Quantification of inflammatory cytokines by Enzyme-Linked Immunosorbent Assay (ELISA).

Levels of tumor necrosis factor alpha (TNF- α), interferon gamma (IFN- γ) and interleukin-8 (IL-8) and 2 (IL-2) were quantified 24 hours after the end of the exposures in the supernatant of cells incubated or not with PMA (5 nM; 24 hours). TNF- α , IFN- γ and IL-8 were quantified using ELISA Ready-SET-GO-2nd Generation (Analytical sensitivity: 4 pg/mL, 4 pg/mL, and 2 pg/mL, respectively; Invitrogen, Carlsbad, CA, USA). IL-2 was quantified using BD OptEIA kit (Analytical sensitivity: 7,8 pg/mL BD Biosciences, San Jose, CA, USA). The procedures were performed according to the manufacturer's instructions.

Intracellular and nuclear staining

Activation of the nuclear factor kappa B (NF κ B) and of extracellular-signal-regulated kinases (ERK) pathway and expression of metallothionein I and II (MT I and II) and 8-hydroxy-2'-deoxyguanosine (8-OHdG) formation in exposed Jurkat cells were assessed by flow cytometry. After the end of exposures, cells were treated or not with PMA (5 nM) for 30 minutes to quantify activation of NF κ B, for 15 minutes to measure the phosphorylation of ERK and for 24 hours to determine the expressions of MT I and II and 8-OHdG. For analysis, the exposed cells were subjected to the same processes. Briefly, cells

were fixed with FACS Lysing (BD Biosciences, San Jose, CA, USA) for 20 minutes at room temperature, then washed with 0.1 M glycine and with PBS containing 1% bovine serum albumin (BSA; Sigma-Aldrich). Cells were permeabilized with 0.1% Triton-100X (Sigma-Aldrich) (0.001% Triton-100X for analysis of MT I and II) for 30 minutes at room temperature. After the permeabilization process, cells were incubated with anti-NFκB-p65 conjugated with allophycocyanin (APC; 1:150; BioLegend, CA, USA), or with anti-ERK1/2 (1:200), anti-phospho ERK (1:100), anti-metallothionein I/II (1:200) or anti-DNA/RNA damage (1:200) purified primary antibodies (Abcam, Cambridge, UK) overnight at 4°C. After incubations, cells were washed with PBS containing 0.1% BSA and incubated with secondary antibodies conjugated with phycoerythrin (PE), fluorescein isothiocyanate (FITC) or AlexaFluor 647 (all diluted at 1:200; Abcam, Cambridge, UK) for 1 hour at room temperature. Lastly, 10,000 events were recorded by flow cytometry (Accuri C6; Becton Dickinson, USA). Data were presented as the median intensity of fluorescence (MFI). For ERK phosphorylation, data were presented as the ratio of p-ERK MFI over total ERK ½ MFI.

Quantification of metals levels by inductively coupled plasma mass spectrometry (ICP-MS)

Ester-cellulose membrane filters (0.8 µm porosity, 37mm diameter; Millipore, Burlington, MA, EUA) were placed in the exposure chamber and exposed to air, CS and HNBT vapor according to the exposure protocol as described above for Jurkat cells. Filters were carefully removed and digested using a microwave oven (MARS 6) following an acid digestion method. Briefly, 5 mL of ultrapure water (MiliQ) and 5 mL of HNO₃ (Sigma Aldrich, St Louis, MO, USA) were added to vessels containing the exposed filters for 25 minutes (15 minutes at ramp stage and 10 minutes on hold at 180 °C). Then, 5 mL of ultrapure water were added and the concentration of metals (Mn, Al, Cr, Fe, Ni, Cu, Zn, As, Cd) was quantified via ICP-MS (Agilent Technologies, Santa Clara, CA, USA).

Animals

Male C57Bl/6 mice (8-weeks old) were bred in a specific pathogen-free animal facility at the School of Medicine of Ribeirao Preto, University of Sao Paulo under controlled temperature and light conditions and given feed and water *ad libitum*. All animal husbandry procedures were in accordance with the guidelines of the Animal Ethics Committee of the School of Medicine of Ribeirao Preto, University of São Paulo (number 563/2019).

Mice exposure to air, HNBT vapor and CS

Mice were exposed to air, cigarette smoke (Marlboro Red, Phillip Morris), or heated tobacco vapor (IQOS, Phillip Morris International) under the Health Canada Intensive (HCI) smoking regime (55mL of smoke during a 2 seconds puffing, every 30 seconds; Health Canada, 1999). An exposure machine was designed (Bonther, Ribeirao Preto, SP, Brazil) allowing for simultaneous exposure of all experimental groups under controlled humidity, temperature, and constant air exhausting to avoid mice intoxication. Cigarette smoke and heated tobacco vapor generated by the heatsticks were aspirated by a vacuum pump and delivered to the exposure chambers. Mice were exposed for 1 hour, twice a day, for 5 days to simulate the cigarette smoke consumption of heavy smokers (Wilson et al., 1992). The

number of cigarettes and heatsticks used was matched by the amount of nicotine for each hour of exposure. A total of 12 conventional cigarettes and 24 heatsticks were used. The mice were euthanized 16 hours after the last exposure for liver and lung removal.

Metallothionein I and II immunohistochemical staining

The day after the last exposure, mice were euthanized and samples of lung and liver were collected and fixed in 4% paraformaldehyde for 24 hours, dehydrated in graded ethanol and embedded in paraffin for immunohistochemical analyses. Lung and liver sections (5µm thickness) were deparaffinized, hydrated, and incubated with sodium citrate buffer (0,1M; pH 6.0) at 96 °C for 30 minutes for antigen retrieval. Endogenous peroxidase activity was blocked with 3% hydrogen peroxide used in three 10 minutes rounds. Next, blockade of unspecific binding sites was carried out with 10% bovine serum albumin (BSA) diluted in Tris-buffer saline (TBS) for one hour. The sections were incubated with purified anti-MT I and II (1:250; ABCAM. Cambridge, UK) overnight at 4 °C. Sections were then washed and incubated with a secondary antibody conjugated with HRP for one hour at room temperature (1:200, ABCAM. Cambridge, UK). Staining was detected using 3,3'-diaminobenzidine (DAB substrate; Invitrogen, USA). The sections were counterstained with hematoxylin, mounted and analyzed. Average DAB intensities were analyzed using the ImageJ software (National Institute of Health, USA).

Data analysis

Statistical analyses were performed using one-way analysis of variance (ANOVA), followed by *post hoc* comparisons using Tukey test. The values are presented as mean ± standard error of mean. Analyses were performed using GraphPad Prism version 7.0 (GraphPad Software, CA, USA).

275 RESULTS

276

277 CS and HNBT exposures decrease cell viability by necrosis

278 Using double staining with annexin V and propidium iodide, we assessed the cytotoxic effects on
 279 Jurkat T cells 24 hours after exposures, assessing not only the number of viable cells but also when
 280 whether they suffered apoptosis or necrosis. CS and HNBT caused cell death mainly by necrosis
 281 (representative dot plots in [Suppl. figure 2.](#)). The effects caused by CS were more intense than those
 282 evoked by HNBT ([Figure 1](#)). It is noteworthy to mention that CS exposure caused an effect related to
 283 exposure times; an exposure time to CS of 30 minutes was chosen for further experiments as it caused
 284 about 20% of cell death ([Suppl. figure 3](#)).

285

286 CS exposure evokes oxygen and nitrogen reactive species production and causes oxidative DNA 287 damage

288 A toxic hallmark of CS is the generation of ROS, which leads to oxidative damage in cells, such as on
 289 membranes, organelles, and DNA (Kamat 2000). PMA is a liposoluble direct activator of intracellular
 290 protein kinase C, triggering NFκB translocation into the nucleus and activation of p47phox and
 291 NADPH oxidase (NOX), leading to activation of the oxidative burst and secretion of cytokines (Min et
 292 al. 2005). Therefore, we here investigated the ability of CS and HNBT to affect ROS generation caused
 293 by PMA. PMA treatment was efficient in inducing the release of ROS by Jurkat cells, and this effect
 294 was not modified in cells exposed to air or HNBT. Nevertheless, CS caused ROS production regardless
 295 of any previous stimulation, which was higher after PMA stimulation ([Figure 2A](#)).

296 NO is a gas produced by isoforms of NO synthases (NOS), and exacerbated production of the
 297 gas occurs by activation of inducible NOS during inflammation (Tousoulis et al. 2012). The reaction
 298 between ROS and NO in the inflamed microenvironment leads to formation of peroxynitrite, a
 299 powerful cytotoxic agent (Radi 2018). Data presented in [Figure 2B](#) shows that only CS was able to
 300 evoke NO production in non- and PMA-stimulated cells.

301 A high concentration of reactive species leads to the formation of 8-OHdG, one of the most
 302 important DNA lesions formed in response to oxidative stress and widely used as a reliable biomarker
 303 to assess oxidative damage (Cao et al. 2016). Data presented in [Figure 3C](#) shows that CS exposure
 304 induced 8-OHdG formation in Jurkat cells, independent of PMA stimuli. Formation of 8-OHdG in cells
 305 exposed to HNBT vapor was equivalent to that detected in cells exposed to air only.

306

307 CS releases higher metals levels than HNBT

308 The activation of the oxidative burst is highly influenced by metals (Nuran et al. 2001), which are toxic
 309 components of CS. A recent publication showed significant amount of metals in HNBT sticks (Koutela
 310 et al, 2020), however no evidence is available regarding the amount released in the IQOS vapor.
 311 Therefore, to better understand the mechanisms of oxidative burst caused by tobacco compounds, we
 312 here investigated the delivery of metals into the exposure chamber by CS and HNBT vapor. Data
 313 obtained showed lower amounts of iron, copper, chromium, aluminum, arsenic and nickel in HNBT

than in CS samples, and no detectable levels of cadmium and manganese in HNBT samples (Figure 3A- F).

CS induces MT I and II expression

Considering the content of metals and generation of oxidative stress caused by CS exposure, we investigated whether exposures to CS or HNBT vapor could evoke MT expression on Jurkat T cells. MT are cysteine-rich low-weight house-keeping proteins expressed to act as free radical scavengers, to protect cell integrity and to rescue homeostasis (Ruttkey-Nedecky et al. 2013). They are rapidly induced by heavy and trace metals, inflammatory cytokines, and ROS (Laukens et al. 2009). Figure 4A shows higher expression of MTs on CS-exposed Jurkat T cells than in counterpart cells exposed to air or HNBT vapor. The same effect was also observed in mice exposed to CS, HNBT vapor or air. The expression of MT was markedly enhanced in liver and lung tissues collected from mice exposed to CS in comparison to tissues obtained from mice exposed to air or HNBT vapor (Figure 4B-G). It is noteworthy to mention that in these tissues MT were not expressed by T lymphocytes (data not shown), as mice were not subjected to local or systemic inflammation that could elicit influx of lymphocytes into tissues. The images here presented show CS exposure induces expression of MT by cells other than lymphocytes. MT are expressed by resident lung cells, such as lung epithelial cells, hepatocytes, mast and Kupffer cells, as well as macrophages (Laukens et al., 2009). Therefore, we evidence MT expression is a sensitive biological endpoint for assessment of effects caused by exposure to tobacco products both in *in vivo* and *in vitro* models.

CS exposure causes release of pro-inflammatory cytokines by Jurkat cells and activates NFκB pathway

As previously mentioned, PMA activation causes activation of NFκB, a pivotal transcription factor of inflammation. Here we show only exposure to CS caused NFκB activation without PMA activation, which was not observed in HNBT vapor or air exposed cells. The robust activation caused by PMA in all groups of cells was not increased by any of the exposures (Figure 5A). Activation of ERK is a fundamental pathway for T lymphocyte proliferation and for antigen response (Chen 2016). For this reason, this pathway was investigated and our data showed PMA, as expected, induced ERK phosphorylation. Although they were not statistically significant, values of ERK phosphorylation were reduced in Air, CS or HNBT vapor exposed cells stimulated with PMA (Figure 5B).

The quantification of levels of pro-inflammatory cytokines TNF-α, IFN-γ and IL-8 showed that CS exposure increased their secretions by Jurkat cells (Figure 5C-E); moreover, the secretion of TNF-α evoked by PMA was markedly increased in CS exposed cells (Figure 5C). PMA stimulation caused IL-2 secretion by Jurkat cells exposed to air, which was abrogated in cells exposed to HNBT or CS (Figure 5F). IL-2 is a primordial cytokine on the control of T cell proliferation and on the switch to Treg profile (Ross and Cantrell 2018).

CS, HNBT vapor and nicotine exposures impair Jurkat T cell proliferation

Once we observed that exposure to both CS and HNBT vapor led to a decreased secretion of IL-2, a pivotal cytokine for T cell proliferation and that nicotine is known to disrupt IL-2 secretion (Ouyang et al. 2000), we hypothesized that these exposures could impact the proliferative ability of Jurkat T cells. Monitoring cell proliferation for 72 hours, we observed that cells exposed to CS and HNBT vapor showed an impaired proliferation capacity, even upon PMA stimulation (Figure 6A-B). As expected, the decrease of IL-2 secretion observed 24 hours after CS or HNBT vapor exposures, impacted the proliferation rate of Jurkat T cells. It is important to highlight that HNBT-exposed cells display an accentuated proliferation impairment with or without PMA stimulation, when compared to CS-exposed group. Based in the fact that nicotine plays a suppressive role in IL-2 secretion and cell proliferation (van Dijk et al. 1998), we treated Jurkat T cell with the same concentration of nicotine released by CS and HNBT for 30 minutes. Nicotine concentrations used here did not have a significant cytotoxic effect on Jurkat T cells (Suppl. figure 4); nevertheless, nicotine decreased IL-2 secretion even upon PMA stimulation (6C) and, in accordance with the effects seen for CS and HNBT exposure, nicotine suppressed the proliferation of Jurkat T cells (Figure 6A, C; suppl. figure 5). Addition of rhIL-2 to CS, HNBT vapor or nicotine exposed cells rescued the proliferation of Jurkat cells (Figure 6B-C).

DISCUSSION

The safe application of novel exposure devices of chemical agents in health programs depends on consolidated data about their mechanisms of action obtained in discerning experimental and clinical studies. HNBT products have been claimed as potential agents which can be used to reduce the harm caused by cigarette smoke (CS) (Smith et al. 2016); nevertheless, there is insufficient data to support such proposal. Based on concerns about CS effects on autoimmune diseases and on the fact data of HNBT products on T cells are not available, we here investigated the mechanisms of CS or HNBT vapor on Jurkat cells, a recognized human T cell lineage (Abraham and Weiss 2004).

Data presented herein show the ability of CS to induce greater cell activation than HNBT, suggesting combustible products are the most responsible for triggering T cells response; however, such CS and HNBT vapor exposures impaired T cell proliferation (Figure 7). It is noteworthy to mention that Jurkat cells were exposed to equivalent amounts of nicotine based on the concentration of this alkaloid in CS and HNBT. Nicotine is the best component to match exposures, as CS and HNBT deliver similar quantities (Marlboro Red CS releases 1.07 ± 0.06 mg/cigarette and IQOS 1.1 ± 0.1 mg) (Mallock et al. 2018). Considering the small differences on nicotine content, cells were exposed to 4 conventional cigarettes and 5/6 HNBT sticks.

Identification of cell death mechanisms predicts the toxicity of xenobiotics. Activation of apoptosis pathways leads cells to death, avoiding the perpetuation of hereditary cell damage and the release of intracellular aggressive compounds to the host microenvironment (Martinvalet et al. 2005). Conversely, death by necrosis damages cell membrane and releases nuclear and cytoplasmic contents harmful to tissues (Rock and Kono 2008). Our data show both CS and HNBT exposures caused cell death, which was more intense in CS exposed cells, mainly by necrosis. Indeed, a previous study using epithelial lung cells, endothelial cells and Jurkat cells showed CS exposure inhibits apoptosis, and the

resulting cell death by necrosis was implicated as a mechanism of loss of alveolar epithelium and lung inflammation in smokers (Wickenden 2003).

Activation of ROS is an efficient mechanism of defense against aggression from different sources. During homeostasis, ROS levels are regulated by various antioxidant systems, and imbalance between free radical and antioxidant machinery causes oxidative stress related to activation of inflammatory pathways and oxidative DNA damage (Mittal et al. 2013). Activation of ROS is a known mechanism of CS toxicity (Chen et al. 2015), which was here corroborated in Jurkat cells. Moreover, exacerbated ROS production in CS exposed cells was detected after stimulation with PMA, a recognized activator of NOX, showing CS exposure primes Jurkat cells for ROS production. These effects were not detected in HNBT vapor exposed cells, despite the fact HNBT products can generate ROS had already been demonstrated in human bronchial epithelial cells (Malinska et al. 2018).

A pattern for NO generation similar to that observed for ROS production also took place after exposures to CS or HNBT, which is dependent on activation of intracellular NO enzymes (NOS) (Murad 2004). NO is a pivotal vessel protector when produced by endothelial and neuronal isoforms of NOS; conversely, higher amounts of NO produced by inducible NOS acts as pro-inflammatory agent (Tousoulis et al. 2012). In this context, the harmful impairment of NO protection on the vessels of smokers causing lung and cardiovascular complications has already been shown (Su et al. 1998). Here we show that CS exposure enhanced NO production by Jurkat cells, which is due to activation of inducible NO, mediating inflammation.

Conjugation of ROS and NO leads to peroxynitrite formation, an unstable and autoreactive molecule with inherent cytotoxicity (Hayashi et al. 2004). Increased levels of ROS and peroxynitrite provoke peroxidation of DNA bases with consequent formation of 8-OHdG, a standard DNA adduct widely used as a biomarker for evaluating oxidative DNA damage in biological samples, including those from smokers (Cao et al. 2016). Along elevated levels of ROS and NO, CS exposure also caused formation of 8-OHdG in Jurkat cells, which was not detected in HNBT exposed cells. Several compounds in CS are responsible for activation of ROS generation, such as nicotine, benzene and its metabolites, polycyclic aromatic hydrocarbons, and metals (Wooten et al. 2006; Bae et al. 2010; Wang et al. 2019). Previous studies have demonstrated that HNBT present lower levels of the majority of these compounds (Auer et al. 2017). Here we show reduced levels of transition and post transition metals in HNBT vapor in comparison to smoke of conventional cigarettes.

In the same manner, as higher ROS and metal levels were detected in CS than HNBT, we also detected higher expression of MT in Jurkat cells and also in cells of lungs and liver of mice exposed to CS. Data here obtained corroborate the higher expression of these proteins in biological samples of smoker patients (Billatos et al. 2018). Although MTs are scavenger of metals and ROS, MT I and II expressions are also associated to the genesis of immune diseases and cancer. MTs induce proliferation, activation, and switch of T cells in different conditions (Subramanian and Deepe 2017), impair IL-27 induced type 1 cell regulatory differentiation involved in autoimmunity modulation (Wu et al. 2013), and shift Th17/Treg balance in rheumatoid arthritis (Sun et al. 2018). Moreover, MT overexpression has been described in several tumor types, and its expression is related to tumor growth and progression, metastasis and drug resistance (Si and Lang 2018). Taken together, it is feasible to

suppose MT may be considered pivotal end points for exposure to tobacco products, and their expressions could be correlated to cell metabolism and functions. In our *in vitro* experimental model, MT I and II were over-expressed in response, at least in part, to ROS and metal aggression in CS exposed cells. Nevertheless, such expression was not enough to counteract the oxidative DNA damage and inflammation caused by CS exposure in Jurkat cells and in mice.

The activation of the NFκB inflammatory pathway has been extensively showed in cells exposed to CS (Anto et al. 2002; Zhang et al. 2016); nevertheless, no data are available regarding HNBT activating NFκB as well as its ability to induce activation of T cells. HNBT vapor did not activate the NFκB pathway in the exposed cells in comparison to the CS-exposed group. While only CS exposure induced pro-inflammatory activation, both CS and HNBT exposures led to a considerable inhibition of IL-2 secretion after PMA activation and consequently decreased the proliferative activity of exposed cells. Indeed, addition of rhIL-2 to the culture medium of exposed cells rescued their proliferation, corroborating the toxic effect of CS, HNBT and nicotine on IL-2 mediated proliferation of T cells. IL-2 is produced by CD4⁺ T cells and binds to high-affinity IL-2 receptors expressed by both CD4⁺ and CD8⁺ T cells. IL-2 displays a fundamental role on T cell differentiation and controls cell phenotypes that are dominantly present in sites of infection, autoimmune disease and cancer (Spolski and Leonard 2018). In these contexts, IL-2 induces Treg polarization and proliferation, protecting the development of autoimmune diseases and also favoring proliferation and generation of effector and memory cytotoxic T cells against tumor cells (Orozco et al. 2020). Reduced IL-2 secretion due to *in vivo* and *in vitro* CS exposure had been previously described, and although some studies present controversial data, the majority of them suggest nicotine, by binding to alpha7 nicotinic acetylcholine receptor, is an inhibitor of IL-2 secretion and consequently, impairs cell proliferation (Madretsma et al. 1996; van Dijk et al. 1998; Nizri et al. 2009; Ouyang et al. 2000). Indeed, reduced proliferation and secretion of IL-2 observed in cells exposed to both CS and HNBT vapor were also observed in cells exposed to nicotine, evidencing nicotine is responsible for the toxic effects on IL-2 secretion and cell proliferation. It is known that CS reduces T cell proliferation leading to impaired immune responsiveness against microbes, allergens and also compromising tumor surveillance (Robbins et al., 2008; Hernandez et al., 2013).

Conclusion

Associated, data here presented show CS exposure activates either damaging or protective pathways in T cells, resulting in a clear activation of oxidative and inflammatory pathways, which are related to the development of autoimmune diseases and cancer. As these end points were reduced in HNBT exposed cells, we confirm HNBT tobacco products are toxic, aggressively affecting T lymphocytes, even if HNBT products possess lower levels of combustible products. Our data highlight the severe downregulation of IL-2 and the disruption of T cell proliferation caused by both CS and HNBT exposures, which might implicate in impaired protection exerted by the immune system against self-aggressions and cancer development. The latter effects are associated with nicotine delivery by both CS and HNBT. Considering nicotine is also toxic to systems other than the immune system, the toxicity of HNBT delivery products must be further investigated in *in vitro* and *in vivo* models.

Acknowledgments: The authors thank Agência Nacional de Vigilância Sanitária (Anvisa) for HNBT import permission. Fundação de Amparo à Pesquisa do Estado de São Paulo (FAPESP; research grant 2014/07328-4 and 2019/19573-7) and Conselho Nacional de Desenvolvimento Científico e Tecnológico (CNPq) for MSc fellow support to P. S.

Conflict of Interest

The authors declare that they have no conflict of interest.

REFERENCES

- Abimannan T, Peroumal D, Parida JR, et al. Oxidative stress modulates the cytokine response of differentiated Th17 and Th1 cells. *Free Radic. Biol. Med.* 2016;99:352–63. <https://doi.org/10.1016/j.freeradbiomed.2016.08.026>
- Abraham, R, Weiss, A. Jurkat T cells and development of the T-cell receptor signaling paradigm. *Nat. Rev. Immunol.* 2004; 4: 301–308. <https://doi.org/10.1038/nri1330>
- Alrouji, M., Manouchehrinia, A., Gran, B., & Constantinescu, C. S. (2019). Effects of cigarette smoke on immunity, neuroinflammation and multiple sclerosis. *J. Neuroimmunol.*, 329, 24–34. <https://doi.org/10.1016/j.jneuroim.2018.10.004>
- Anto RJ. Cigarette smoke condensate activates nuclear transcription factor- kappaB through phosphorylation and degradation of IkappaBalpha: correlation with induction of cyclooxygenase-2. *Carcinogenesis* 2002;23:1511–8. <http://doi.org/10.1093/carcin/23.9.1511>
- Auer R, Concha-Lozano N, Jacot-Sadowski I, et al. Heat-Not-Burn Tobacco Cigarettes. Smoke by any other name. *JAMA Intern. Med.* 2017;177:1050-2. <http://doi.org/10.1001/jamainternmed.2017.1419>
- Azzopardi D, Haswell LE, Foss-Smith G, et al. Evaluation of an air–liquid interface cell culture model for studies on the inflammatory and cytotoxic responses to tobacco smoke aerosols. *Toxicol. in Vitro* 2015;29:1720–8. <http://doi.org/10.1016/j.tiv.2015.06.016>
- Bae S, Pan X-C, Kim S-Y, et al. Exposures to Particulate Matter and Polycyclic Aromatic Hydrocarbons and Oxidative Stress in Schoolchildren. *Environ. Health Perspect.* 2010;118:579–83. <http://doi.org/10.1289/ehp.0901077>

- 513 Bentley MC, Almstetter M, Arndt D. et al. Comprehensive chemical characterization of the aerosol
 514 generated by a heated tobacco product by untargeted screening. *Anal. Bioanal Chem.* 2020; 412:2675-
 515 85. <http://doi.org/10.1007/s00216-020-02502-1>
 516
- 517 Benowitz, N. L., & Gourlay, S. G. (1997). Cardiovascular Toxicity of Nicotine: Implications for
 518 Nicotine Replacement Therapy. *J. Am. Coll. Cardiol.*, 29(7), 1422–1431.
 519 [https://doi.org/10.1016/s0735-1097\(97\)00079-x](https://doi.org/10.1016/s0735-1097(97)00079-x)
 520
- 521 Billatos E, Faiz A, Gesthalter Y, et al. Impact of acute exposure to cigarette smoke on airway gene
 522 expression. *Physiol. Genomics* 2018;50:705–13. <http://doi:10.1152/physiolgenomics.00092.2017>
 523
- 524 Cao C, Lai T, Li M, et al. Smoking-promoted oxidative DNA damage response is highly correlated to
 525 lung carcinogenesis. *Oncotarget* 2016;7:18919-26. <http://doi:10.18632/oncotarget.7810>
 526
- 527 Chen SS, Hu Z, Zhong X-P. Diacylglycerol Kinases in T Cell Tolerance and Effector Function. *Front.*
 528 *Cell Dev. Biol.* 2016;4:130. <http://doi:10.3389/fcell.2016.00130>
 529
- 530 Chen Z, Wang D, Liu X, et al. Oxidative DNA damage is involved in cigarette smoke-induced lung
 531 injury in rats. *Environ. Health Prev. Med.* 2015;20:318–24. <http://doi:10.1007/s12199-015-0469-z>
 532
- 533 Forster M, Fiebelkorn S, Yurteri C, et al. Assessment of novel tobacco heating product THP1.0. Part 3:
 534 Comprehensive chemical characterisation of harmful and potentially harmful aerosol emissions. *Regul.*
 535 *Toxicol. Pharm.* 2018;93:14–33. <http://doi:10.1016/j.yrtph.2017.10.006>
 536
- 537 Ghoshal K, Jacob ST. Regulation of metallothionein gene expression. In: *Prog Nucleic Acid Res Mol*
 538 *Biol.* Elsevier 2001; 66:357–84. [http://doi:10.1016/s0079-6603\(00\)66034-8](http://doi:10.1016/s0079-6603(00)66034-8)
 539
- 540 Gonçalves RB, Coletta RD, Silvério KG, et al. Impact of smoking on inflammation: overview of
 541 molecular mechanisms. *J. Inflamm. Res.* 2011;60:409–24. <http://doi:10.1007/s00011-011-0308-7>
 542
- 543 Hayashi Y, Sawa Y, Nishimura M, et al. Peroxynitrite, a product between nitric oxide and superoxide
 544 anion, plays a cytotoxic role in the development of post-bypass systemic inflammatory response. *Eur.*
 545 *J. Cardiothorac. Surg.* 2004;26:276–80. <http://doi:10.1016/j.ejcts.2004.03.033>
 546
- 547 Health Canada, H., Health Canada Test Method T-115, Determination of “Tar” and Nicotine in
 548 Sidestream Tobacco Smoke. 1999.
 549
- 550 Hecht SS. Lung carcinogenesis by tobacco smoke. *Int J Cancer*, 2012;131:2724–32. <http://doi:10.1002/ijc.27816>
 551
 552

- Heluany CS, Kupa LVK, Viana MN, et al. Hydroquinone exposure worsens the symptomatology of rheumatoid arthritis. *Chem-Biol Interact.* 2018;291:120–7. <http://doi:10.1016/j.cbi.2018.06.016>
- Hernandez CP, Morrow K, Velasco C, Wyczzechowska DD, Naura AS, Rodriguez PC. Effects of cigarette smoke extract on primary activated T cells. *Cellular Immunology.* 2013; 282:38–43. Available at: <http://doi:10.1016/j.cellimm.2013.04.005>.
- IARC (2004) Tobacco smoke and involuntary smoking. *IARC Monogr Eval Carcinog Risks Hum* 83:1–1438
- Kamat J. Reactive oxygen species mediated membrane damage induced by fullerene derivatives and its possible biological implications. *Toxicology* 2000;155:55–61. [http://doi:10.1016/s0300-483x\(00\)00277-8](http://doi:10.1016/s0300-483x(00)00277-8)
- Koch A, Gaczowski M, Sturton G, et al. Modification of surface antigens in blood CD8+ T-lymphocytes in COPD: effects of smoking. *Eur. Respir. J.* 2006;29:42–50. <http://doi:10.1183/09031936.00133205>
- Koutela, N., Fernández, E., Saru, M.-L., & Psillakis, E. (2020). A comprehensive study on the leaching of metals from heated tobacco sticks and cigarettes in water and natural waters. *Sci. Total. Environ.*, 714, 136700. <https://doi.org/10.1016/j.scitotenv.2020.136700>
- Laukens D, Waeytens A, De Bleser P, et al. Human Metallothionein Expression under Normal and Pathological Conditions: Mechanisms of Gene Regulation Based on in silico Promoter Analysis. *Crit Rev Eukar Gene.* 2009;19:301–17. <http://doi:10.1615/critreveukargeneexpr.v19.i4.40>
- Leigh NJ, Tran PL, O'Connor RJ, et al. Cytotoxic effects of heated tobacco products (HTP) on human bronchial epithelial cells. *Tob. Control* 2018;27:s26–9. <http://doi:10.1136/tobaccocontrol-2018-054317>
- Mainali, P., Pant, S., Rodriguez, A. P., Deshmukh, A., & Mehta, J. L. (2014). Tobacco and Cardiovascular Health. *Cardiovasc. Toxicol.*, 15(2), 107–116. <http://doi.org/10.1007/s12012-014-9280-0>
- Malinska D, Szymański J, Patalas-Krawczyk P, et al. Assessment of mitochondrial function following short- and long-term exposure of human bronchial epithelial cells to total particulate matter from a candidate modified-risk tobacco product and reference cigarettes. *Food Chem. Toxicol.* 2018;115:1–12. doi: <http://10.1016/j.fct.2018.02.013>

- 592 Mallock N, Böss L, Burk R, et al. Levels of selected analytes in the emissions of “heat-not-burn”
 593 tobacco products that are relevant to assess human health risks. *Arch. Toxicol.* 2018;92:2145–9. doi:
 594 [http:// 10.1007/s00204-018-2215-y](http://10.1007/s00204-018-2215-y)
 595
- 596 Martinvalet D, Zhu P, Lieberman J. Granzyme A Induces Caspase-Independent Mitochondrial
 597 Damage, a Required First Step for Apoptosis. *Immunity* 2005;22:355–70. [http://](http://doi:10.1016/j.immuni.2005.02.004)
 598 doi:10.1016/j.immuni.2005.02.004
 599
- 600 Mittal M, Siddiqui MR, Tran K, et al. Reactive Oxygen Species in Inflammation and Tissue Injury.
 601 *Antioxid Redox Signal.* 2014;20:1126–67. [http:// doi:10.1089/ars.2012.5149](http://doi:10.1089/ars.2012.5149)
 602
- 603 Min J-K, Kim Y-M, Kim SW, et al. TNF-Related Activation-Induced Cytokine Enhances Leukocyte
 604 Adhesiveness: Induction of ICAM-1 and VCAM-1 via TNF Receptor-Associated Factor and Protein
 605 Kinase C-Dependent NF- κ B Activation in Endothelial Cells. *J Immunol.* 2005;175:531–40. [http://](http://doi:10.4049/jimmunol.175.1.531)
 606 doi:10.4049/jimmunol.175.1.531
 607
- 608 Madretsma GS, Donze GJ, van Dijk APM, et al. Nicotine inhibits the in vitro production of interleukin
 609 2 and tumour necrosis factor- α by human mononuclear cells. *Immunopharmacol.* 1996;35:47–51.
 610 [http:// doi:10.1016/0162-3109\(96\)00122-1](http://doi:10.1016/0162-3109(96)00122-1)
 611
- 612 Murad F. Discovery of Some of the Biological Effects of Nitric Oxide and its Role in Cell Signaling.
 613 *Biosci Rep.* 2004;24:452–74. <http://doi:10.1007/s10540-005-2741-8>
 614
- 615 Neunteufl, T., Heher, S., Kostner, K., Mitulovic, G., Lehr, S., Khoschsorur, G., Schmid, R. W.,
 616 Maurer, G., & Stefenelli, T. (2002). Contribution of nicotine to acute endothelial dysfunction in long-
 617 term smokers. *J. Am. Coll. Cardiol.*, 39(2), 251–256. [https://doi.org/10.1016/s0735-1097\(01\)01732-6](https://doi.org/10.1016/s0735-1097(01)01732-6)
 618
- 619 Nuran Ercal BSP, Hande Gurer-Orhan BSP, Nukhet Aykin-Burns BSP. Toxic Metals and Oxidative
 620 Stress Part I: Mechanisms Involved in Metal induced Oxidative Damage. *Curr Top Med Chem.*
 621 2001;1:529–39. [http:// doi:10.2174/1568026013394831](http://doi:10.2174/1568026013394831)
 622
- 623 Nguyen NT, Nakahama T, Kishimoto T. Aryl hydrocarbon receptor and experimental autoimmune
 624 arthritis. *Semin Immunopathol.* 2013;35:637–44. <http://doi:10.1007/s00281-013-0392-6>
 625
- 626 Nguyen, H. M.-H., Torres, J. A., Agrawal, S., & Agrawal, A. (2020). Nicotine Impairs the Response of
 627 Lung Epithelial Cells to IL-22. *Mediators Inflamm.*, 2020, 1–9. <https://doi.org/10.1155/2020/6705428>
 628
- 629 Nizri E, Irony-Tur-Sinai M, Lory O, et al. Activation of the Cholinergic Anti- Inflammatory System by
 630 Nicotine Attenuates Neuroinflammation via Suppression of Th1 and Th17 Responses. *J Immunol.*
 631 2009;183:6681–8. [http:// doi:10.4049/jimmunol.0902212](http://doi:10.4049/jimmunol.0902212)

- 632
- 633 Orozco Valencia A, Camargo Knirsch M, Suavinho Ferro E, et al. Interleukin-2 as immunotherapeutic
 634 in the autoimmune diseases. *Int. Immunopharmacol.* 2020;81:106296.
 635 <http://doi:10.1016/j.intimp.2020.106296>
 636
- 637 Ouyang Y, Virasch N, Hao P, et al. Suppression of human IL-1 β , IL-2, IFN- γ , and TNF- α production
 638 by cigarette smoke extracts. *J. Allergy Clin. Immunol.* 2000;106:280–7. [http://](http://doi:10.1067/mai.2000.107751)
 639 doi:10.1067/mai.2000.107751
 640
- 641 Pfeifer, G, Denissenko, M, Olivier, M. et al. Tobacco smoke carcinogens, DNA damage and p53
 642 mutations in smoking-associated cancers. *Oncogene* 21, 7435–7451 (2002). [http://](http://doi.org/10.1038/sj.onc.1205803)
 643 doi.org/10.1038/sj.onc.1205803
 644
- 645 Radi R. Oxygen radicals, nitric oxide, and peroxynitrite: Redox pathways in molecular medicine. *Proc.*
 646 *Natl. Acad. Sci. USA* 2018;115:5839–48. <http://doi:10.1073/pnas.1804932115>
 647
- 648 Robbins, C.S., Franco, F., Mouded, M., Cernadas, M. and Shapiro, S.D. (2008) Cigarette Smoke
 649 Exposure Impairs Dendritic Cell Maturation and T Cell Proliferation in Thoracic Lymph Nodes of
 650 Mice. *The Journal of Immunology*, 180, 6623–6628. <http://doi.org/10.4049/jimmunol.180.10.6623>.
 651
- 652 Ruttkay-Nedecky B, Nejdil L, Gumulec J, et al. The Role of Metallothionein in Oxidative Stress. *Int. J.*
 653 *Mol. Sci.* 2013;14:6044–66. [http:// doi:10.3390/ijms14036044](http://doi:10.3390/ijms14036044)
 654
- 655 Rock KL, Kono H. The Inflammatory Response to Cell Death. *Annu Rev Pathol Mech.*2008;3:99–126.
 656 <http://doi:10.1146/annurev.pathmechdis.3.121806.151456>
 657
- 658 Ross SH, Cantrell DA. Signaling and Function of Interleukin-2 in T Lymphocytes. *Annu. Rev.*
 659 *Immunol.* 2018;36:411–33. <http://doi:10.1146/annurev-immunol-042617-053352>
 660
- 661 Rubin DT, Hanauer SB. Smoking and inflammatory bowel disease. *Eur J Gastroen Hepat*
 662 2000;12:855–62. <http://doi:10.1097/00042737-200012080-00004>
 663
- 664 Qiu F, Liang C-L, Liu H, et al. Impacts of cigarette smoking on immune responsiveness: Up and down
 665 or upside down? *Oncotarget* 2016;8. <http://doi:10.18632/oncotarget.13613>
 666
- 667 Si M, Lang J. The roles of metallothioneins in carcinogenesis. *J. Hematol Oncol.* 2018;11:107.
 668 <http://doi:10.1186/s13045-018-0645-x>
 669

- 670 Śliwińska-Mossoń, M., & Milnerowicz, H. (2017). The impact of smoking on the development of
 671 diabetes and its complications. *Diabetes Vasc. Dis. Res.*, 14(4), 265–276.
 672 <https://doi.org/10.1177/1479164117701876>
 673
- 674 Smith MR, Clark B, Lüdicke F, et al. Evaluation of the Tobacco Heating System 2.2. Part 1:
 675 Description of the system and the scientific assessment program. *Regul. Toxicol. Pharm.* 2016;81:S17–
 676 26. <http://doi:10.1016/j.yrtph.2016.07.006>
 677
- 678 Sohal SS, Eapen MS, Naidu VGM, et al. IQOS exposure impairs human airway cell homeostasis:
 679 direct comparison with traditional cigarette and e-cigarette. *ERJ Open Research* 2019;5 pii: 00159-
 680 2018. <http://doi:10.1183/23120541.00159-2018>
 681
- 682 Spolski R, Li P, Leonard WJ. Biology and regulation of IL-2: from molecular mechanisms to human
 683 therapy. *Nat. Rev. Immunol.* 2018;18:648–59. <http://doi:10.1038/s41577-018-0046-y>
 684
- 685 St.Helen G, Jacob III P, Nardone N, et al. IQOS: examination of Philip Morris International's claim of
 686 reduced exposure. *Tob. Control* 2018;27:s30–6. <http://doi:10.1136/tobaccocontrol-2018-054321>
 687
- 688 Stabbert, R., Dempsey, R., Diekmann, J., Euchenhofer, C., Hagemeister, T., Haussmann, H.-J., ...
 689 Veltel, D. J. (2017). Studies on the contributions of smoke constituents, individually and in mixtures, in
 690 a range of in vitro bioactivity assays. *Toxicol. in Vitro*, 42, 222–246.
 691 <https://doi.org/10.1016/j.tiv.2017.04.003>
 692
- 693 Su Y, Han W, Giraldo C, et al. Effect of Cigarette Smoke Extract on Nitric Oxide Synthase in
 694 Pulmonary Artery Endothelial Cells. *Am. J. Resp. Cell Mol.* 1998;19:819–25.
 695 <http://doi:10.1165/ajrcmb.19.5.3091>
 696
- 697 Subramanian Vignesh K, Deepe Jr. G. Metallothioneins: Emerging Modulators in Immunity and
 698 Infection. *Int. J. Mol. Sci.* 2017;18:2197. <http://doi:10.3390/ijms18102197>
 699
- 700 Sun J, Li L, Li L, et al. Metallothionein-1 suppresses rheumatoid arthritis pathogenesis by shifting the
 701 Th17/Treg balance. *Eur. J. Immunol.* 2018;48:1550–62. <http://doi:10.1002/eji.201747151>
 702
- 703 Sun, L., Wang, X., Gu, T., Hu, B., Luo, J., Qin, Y., & Wan, C. (2020). Nicotine triggers islet β cell
 704 senescence to facilitate the progression of type 2 diabetes. *Toxicology*, 441, 152502.
 705 <https://doi.org/10.1016/j.tox.2020.152502>
 706
- 707 Suzuki, K., Washio, T., Tsukamoto, S., Kato, K., Iwamoto, E., & Ogoh, S. (2020). Habitual cigarette
 708 smoking attenuates shear - mediated dilation in the brachial artery but not in the carotid artery in
 709 young adults. *Physiol. Rep.*, 8(3). <https://doi.org/10.14814/phy2.14369>

- 710
 711 Talbot J, Peres RS, Pinto LG, et al. Smoking-induced aggravation of experimental arthritis is
 712 dependent of aryl hydrocarbon receptor activation in Th17 cells. *Arthritis Res. Ther.* 2018;20.
 713 <http://doi:10.1186/s13075-018-1609-9>
 714
 715 Tousoulis D, Kampoli A-M, Tentolouris Nikolaos Papageorgiou C, et al. The Role of Nitric Oxide on
 716 Endothelial Function. *Cur. Vasc Pharmacol.* 2012;10:4–18. <http://doi:10.2174/157016112798829760>
 717
 718 Valavanidis A, Vlachogianni T, Fiotakis K. Tobacco Smoke: Involvement of Reactive Oxygen Species
 719 and Stable Free Radicals in Mechanisms of Oxidative Damage, Carcinogenesis and Synergistic Effects
 720 with Other Respirable Particles. *Int. J. Environ. Res. Public Health* 2009;6:445–62.
 721 <http://doi:10.3390/ijerph6020445>
 722
 723 van Dijk AP, Meijssen MA, Brouwer AJ, et al. Transdermal nicotine inhibits interleukin 2 synthesis by
 724 mononuclear cells derived from healthy volunteers. *Eur J Clin Invest.* 1998;28:664–71.
 725 <http://doi:10.1046/j.1365-2362.1998.00344.x>
 726
 727 Wang, D., Zhou, R., Yao, Y., Zhu, X., Yin, Y., Zhao, G., Dong, N., & Sheng, Z. (2010). Stimulation of
 728 $\alpha 7$ Nicotinic Acetylcholine Receptor by Nicotine Increases Suppressive Capacity of Naturally
 729 Occurring CD4+CD25+ Regulatory T Cells in Mice In Vitro. *J. Pharmacol. Exp. Ther.*, 335(3), 553–
 730 561. <https://doi.org/10.1124/jpet.110.169961>
 731
 732 Wang Z, Liu B, Zhu J, et al. Nicotine-mediated autophagy of vascular smooth muscle cell accelerates
 733 atherosclerosis via nAChRs/ROS/NF- κ B signaling pathway. *Atherosclerosis* 2019;284:1–10.
 734 <http://doi:10.1016/j.atherosclerosis.2019.02.008>
 735
 736 Warren GW, Cummings KM. Tobacco and Lung Cancer: Risks, Trends, and Outcomes in Patients with
 737 Cancer. *J. Clin. Oncol. Educational Book* 2013; :359–64. http://doi:10.14694/edbook_am.2013.33.359
 738
 739 Weyand CM, Goronzy JJ. A Mitochondrial Checkpoint in Autoimmune Disease. *Cell Metab.*
 740 2018;28:185–6. <http://doi:10.1016/j.cmet.2018.07.014>
 741
 742 Wickenden JA, Clarke MCH, Rossi AG, et al. Cigarette Smoke Prevents Apoptosis through Inhibition
 743 of Caspase Activation and Induces Necrosis. *Am. J. Resp. Cell Mol.* 2003;29:562–70.
 744 <http://doi:10.1165/rcmb.2002-0235oc>
 745
 746 Wilson, D., Wakefield, M., Owen, N., & Roberts, L. (1992). Characteristics of heavy smokers. *Prev.*
 747 *Med.*, 21(3), 311–319. [https://doi.org/10.1016/0091-7435\(92\)90030-l](https://doi.org/10.1016/0091-7435(92)90030-l)
 748

Wooten JB, Chouchane S, McGrath TE (2006) Tobacco Smoke Constituents Affecting Oxidative Stress. In: Halliwell B.B., Poulsen H.E. (eds) Cigarette Smoke and Oxidative Stress. Springer, Berlin, Heidelberg

Wu C, Pot C, Apetoh L, et al. Metallothioneins negatively regulate IL-27- induced type 1 regulatory T-cell differentiation. Proc Natl Acad Sci U S A. 2013;110:7802–7. <http://doi:10.1073/pnas.1211776110>
doi:10.1007/3-540-32232-9_2

Zhang C, Qin S, Qin L et al. Cigarette smoke extract-induced p120-mediated NF-κB activation in human epithelial cells is dependent on the RhoA/ROCK pathway. Sci Rep 2016;6: 23131. <http://doi.org/10.1038/srep23131>

FIGURE LEGENDS

Figure 1. CS and HNBT alter cell viability and increase necrosis in Jurkat T cells. Cell viability was evaluated 24 hours after exposures and PMA treatment. Viable cells (A), cells in necrosis (B), apoptosis (C) and late apoptosis (D). Data were obtained by flow cytometry and express mean ± standard error of the mean of 6 experiments. *p<0.05; **p<0.01 vs. respective values in non-PMA treated air exposed cells (control).

Figure 2. CS, but not HNBT, increases oxygen and nitrogen reactive species and oxidative DNA damage 8-OHdG. Oxidative parameters and damage induced by exposures were evaluated 45 minutes after the end of exposures or PMA treatment for ROS production (A), and 24 hours after for NO release (B) and 8-OHdG (C). Data express mean ± standard error of the mean of 5 experiments for each parameter. * p<0.05; **p<0.01, ***<0.001 vs. respective values in air exposed cells; # p<0.05; ##p<0.01; ###p<0.001 vs. respective non-treated cells (control).

Figure 3. CS delivers higher levels of metals to the exposure chamber than HNBT. Heavy metal and transition metal concentrations in the exposure chamber after 30 minutes of exposure (A-H). Data express mean ± standard error of the mean of 3 or 5 experiments, respectively. Metals were analyzed by ICP-MS. * p<0.05; **p<0.01, ***<0.001 vs. airflow control.

Figure 4. CS exposure increases MT I and II expression *in vitro* and *in vivo*. The expression of MT I and II were evaluated in Jurkat T cells (A) and in the lung and liver of mice exposed to air (B-E), HNBT (C-F) and CS (D-G). Mean intensity of pulmonary (I) and hepatic (H) MT I and II expression. Data express mean ± standard error of the mean of 5 experiments. * p<0.05; **p<0.01, ***<0.001 vs. airflow control. n = 5 mice/group. Sections 5µm. Bar: 50µm (B, C and D); 20µm (E, F and G). NC:

negative control of the reaction. Black arrows indicate MT I and II expression. Counterstaining: Hematoxylin.

Figure 5. CS exposure causes pro-inflammatory cytokines release and lead to NF κ B activation. TNF- α (A), IFN- γ (B), IL-8 (C) and IL-2 (D) secretion was measured in the supernatant by ELISA 24 hours after the exposures. NF κ B p65 activity (E) was evaluated 30 minutes after exposures and p-ERK/ERK1/2 (G) 15 minutes after exposures. Data express mean \pm standard error of the mean of 6 experiments. * $p<0.05$; ** $p<0.01$, *** $p<0.001$ vs. respective values in air exposed cells; # $p<0.05$; ## $p<0.01$; ### $p<0.001$ vs. respective non-treated cells (control).

Figure 6. CS, HNBT vapor and nicotine exposure lead to disrupted Jurkat T cell proliferation and exogenous rhIL-2 rescues the proliferative capacity.

Cell proliferation was monitored for 72 hours after exposures and PMA or rhIL-2 treatment. CFSE MFI fold change in Jurkat T cells exposed or not to PMA (A) or rhIL-2 (B) in relation to the MFI for each respective basal group. Representative overlay histograms of CFSE MFI as measured 24, 48 and 72 hours after exposures (C). Data express mean \pm standard error of the mean of 5 experiments. ** $p<0.01$, *** $p<0.001$ vs. respective values in basal group (non- or PMA- or IL-2-stimulated cells); ## $p<0.01$; ### $p<0.001$ vs. respective values in air exposed cells. & $p<0.05$; && $p<0.01$; &&& $p<0.001$ vs. respective non-treated cells (control).

Supplementary Figure 1. Schematic exposure model. Using an air-liquid interface cell culture protocol, Jurkat cells were placed into 12 mm inserts with 0,4 μ m porosity and exposed to CS and HNBT vapor (45 rpm), or airflow (25 rpm). An exposure chamber and peristaltic pumps were used for exposures protocol, as previously described (Azzopardi et al. 2015). Exposure design allows for symmetrical smoke/vapor distribution into the plate and allows a constant medium flow at 20 rpm.

Supplementary Figure 2. Representative dot plots of Annexin V/PI Staining. Raw data representative of the double staining with Annexin V/Propidium Iodide of Jurkat cells exposed to air, HNBT vapor or CS, stimulated or not with PMA.

Supplementary Figure 3. Impact of time-exposure in cell viability and oxidative response. Jurkat cells were exposed to cigarette smoke at different times at 45 rpm of smoke flow to standardize the impact of time of exposure in cell viability (A) 24 hours after exposure and in ROS production (B) 45 minutes after exposure by flow cytometry. The present data show the current protocol performed in all experiments (2s smoke/vapor, followed by 58s of airflow). Higher times of CS exposure (4s, followed by 56s or 2s, followed by 28s of air in 15, 30, 45 or 60 minutes) caused an acute cytotoxic effect (85-100 %; data not shown).

829 **Supplementary Figure 4. Impact of nicotine treatment in cell viability and death.** Jurkat cells were
830 treated to equivalents concentrations of nicotine based on CS and HNBT vapor release. Viable cells
831 (A), Necrotic (B) and early (C) and late apoptosis (D) are represented. Impact of nicotine treatment in a
832 concentration dependent manner in cell viability and death, viable cells (E), Necrotic (F) and early (G)
833 and late apoptosis (H) are represented. Data express mean \pm standard error of the mean of 3
834 experiments. * $p < 0.05$. basal vs. nicotine treated cells.

835

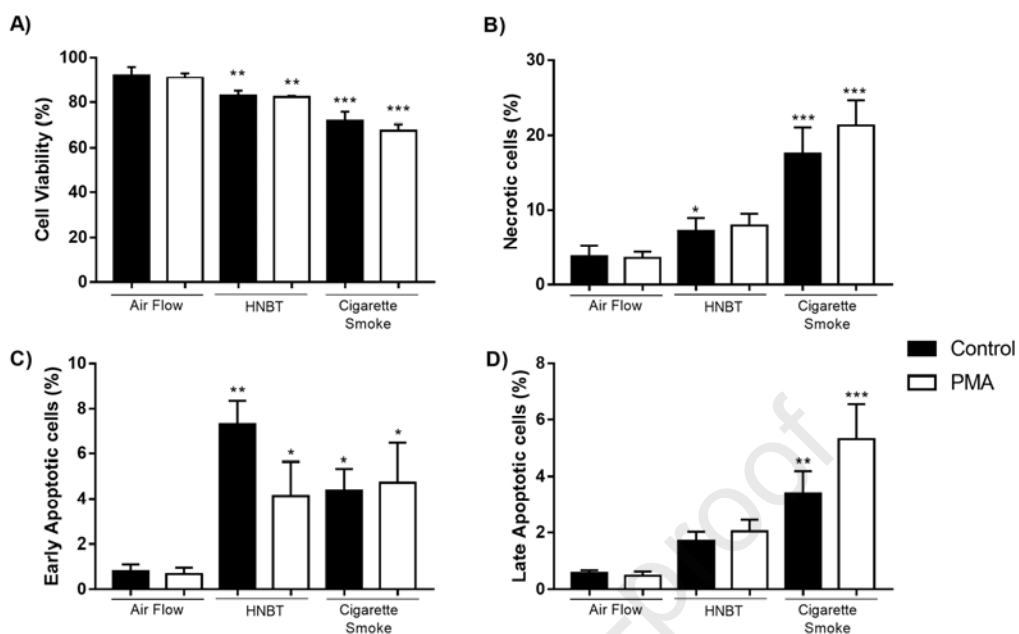
836 **Supplementary Figure 5. Proliferation of Jurkat T cells treated with different nicotine**
837 **concentrations and stimulated or not with PMA.** Cell proliferation was monitored for 72 hours after
838 exposures followed by PMA (5nM) stimulation. CFSE MFI fold change from PMA-stimulated or not
839 Jurkat cells treated with nicotine at different concentrations (A). Representative overlay histograms of
840 CFSE MFI obtained at 24, 48 and 72 hours after exposures (B). Data express mean \pm standard error of
841 the mean of 3 experiments. * $p < 0.01$, *** $p < 0.001$ vs. respective values in basal group (non- or PMA-
842 stimulated cells); ## $p < 0.01$ vs. respective values in non-stimulated cells.

843

844

845

846 Figure 1.



847

848

849

850

851

852

853

854

855

856

857

858

859

860

861

862

863

864

865

866

Figure 2.

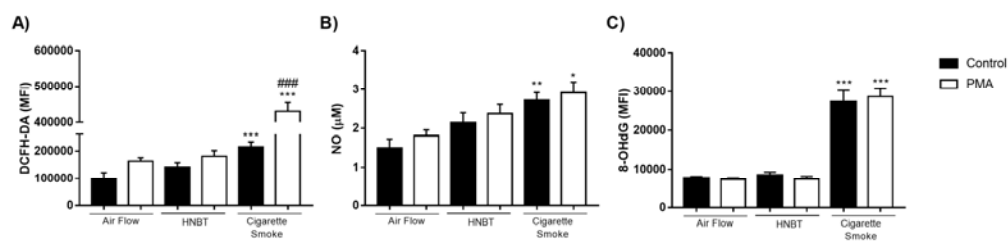


Figure 3.

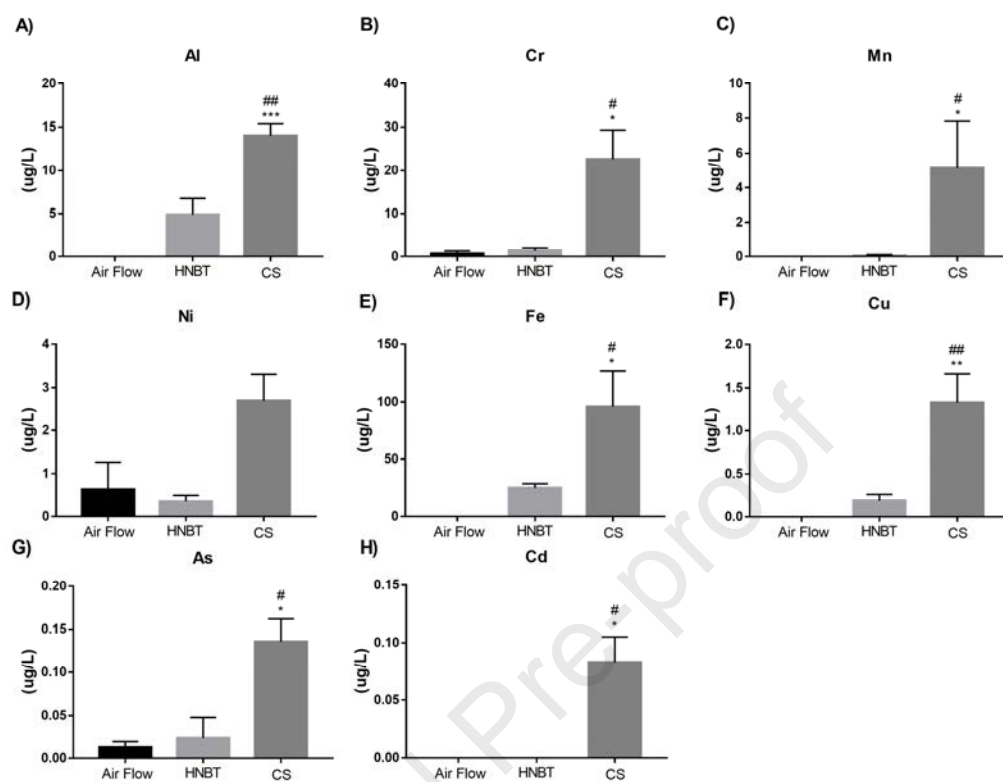
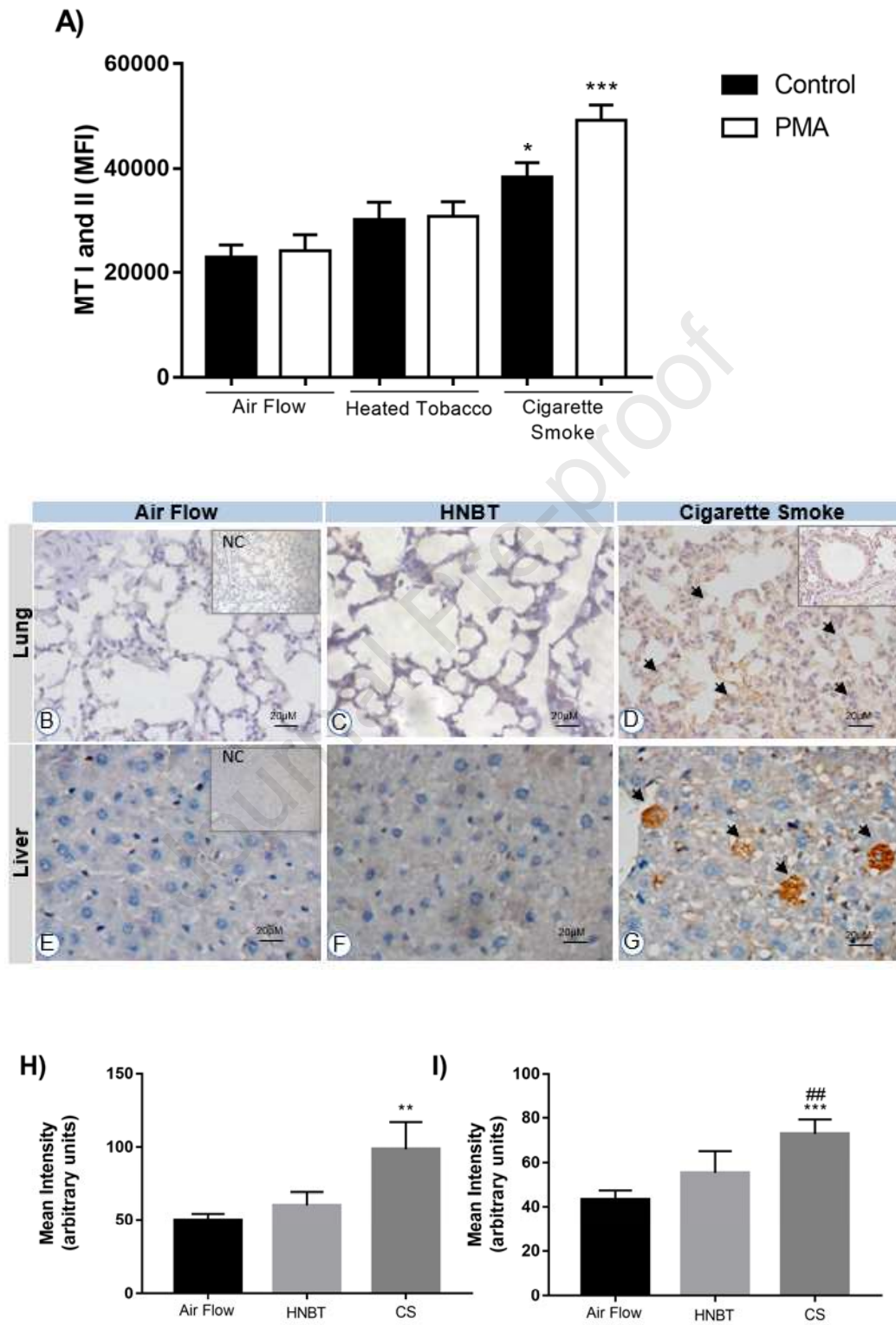
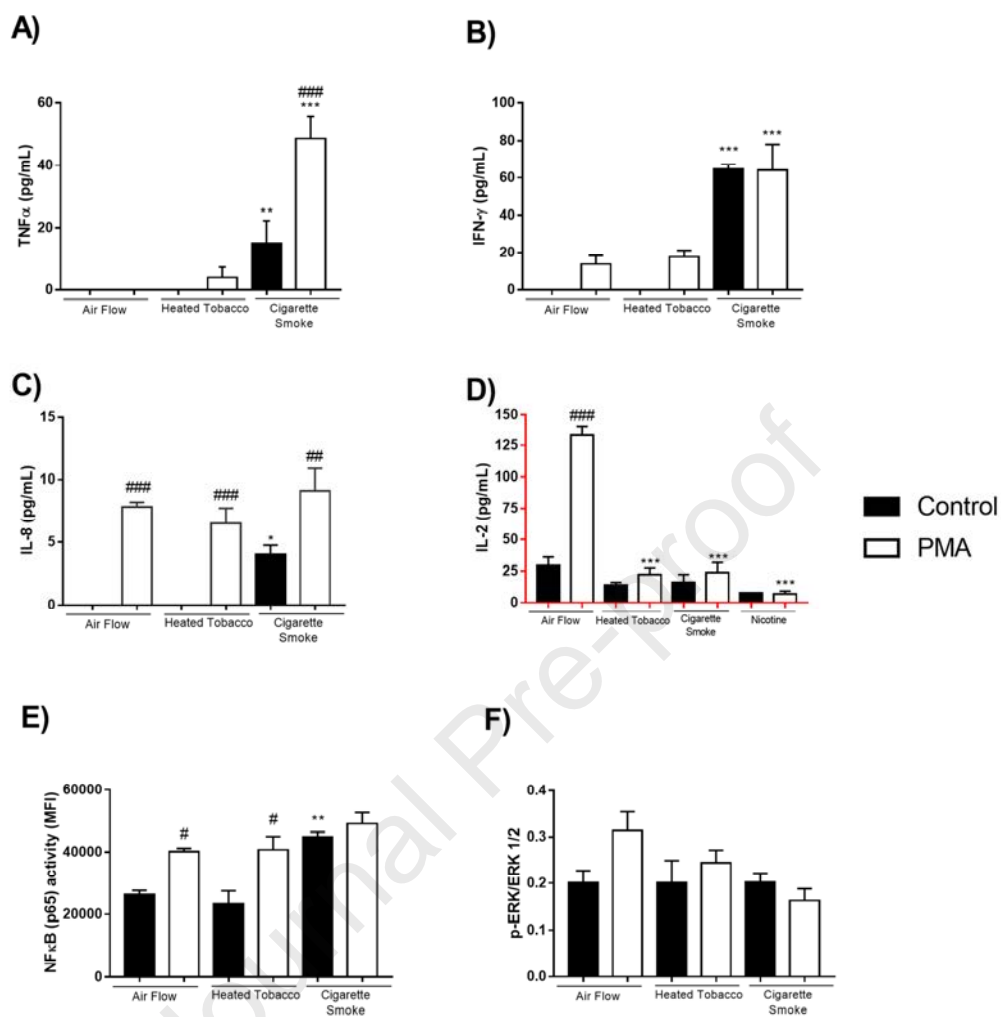


Figure 4.

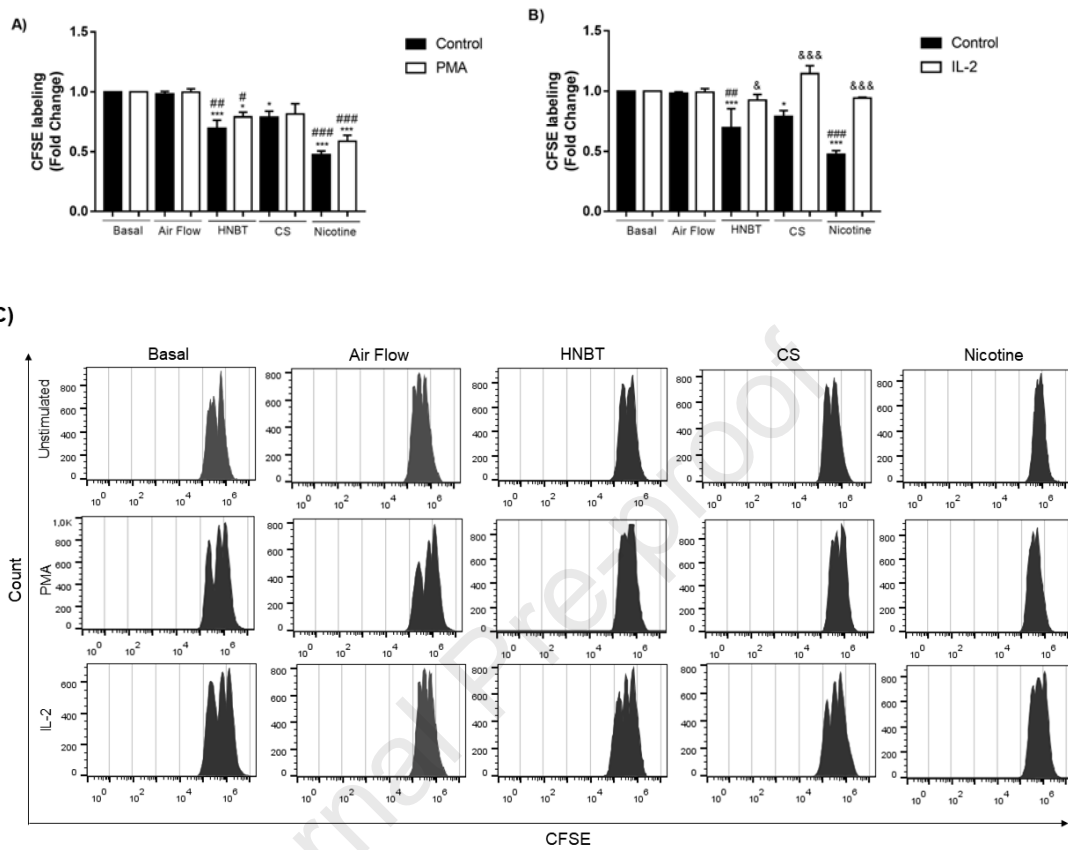


931 Figure 5



932
933
934
935

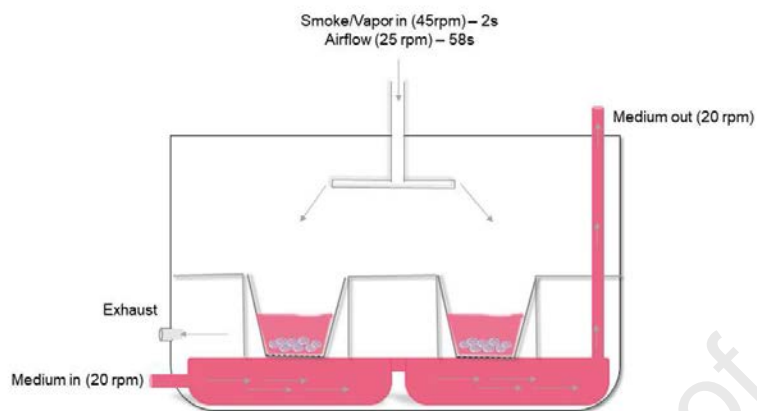
Figure 6.



961 **Supplementary Material**

962

963 Supplementary Figure 1.



964

965

966

967

968

969

970

971

972

973

974

975

976

977

978

979

980

981

982

983

984

985

986

987

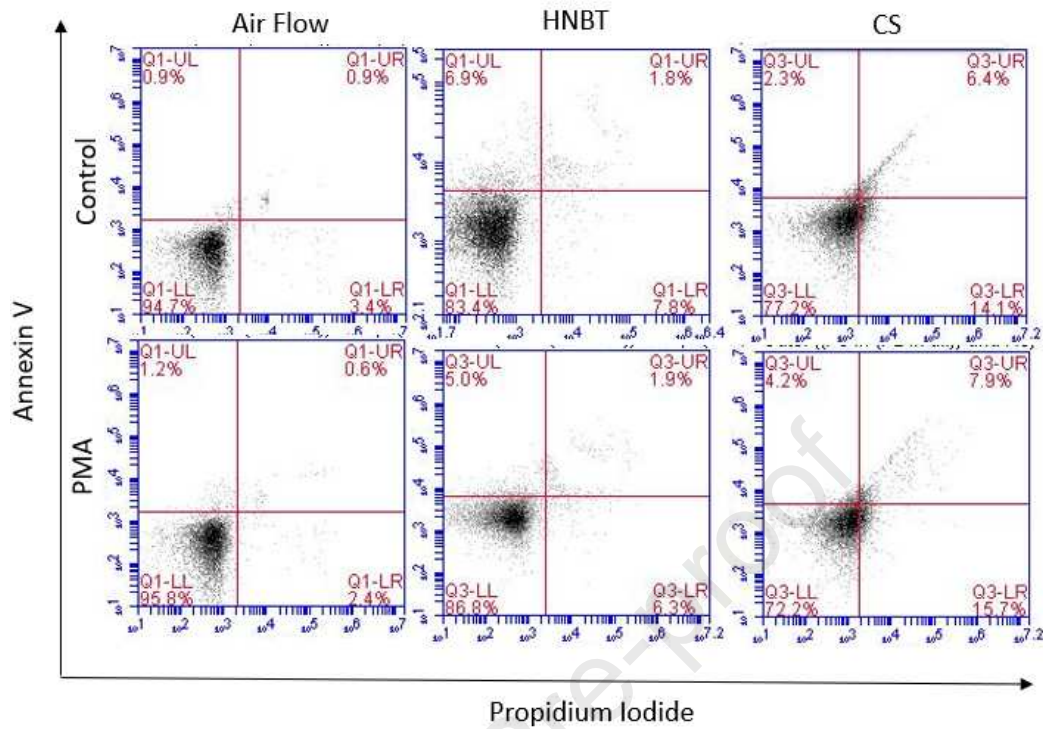
988

989

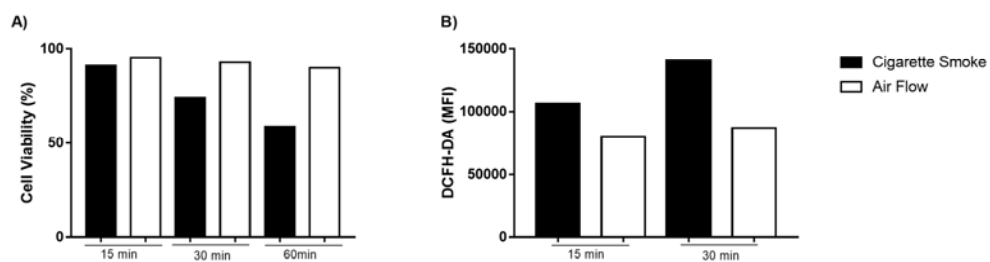
990

991

Supplementary Figure 2.

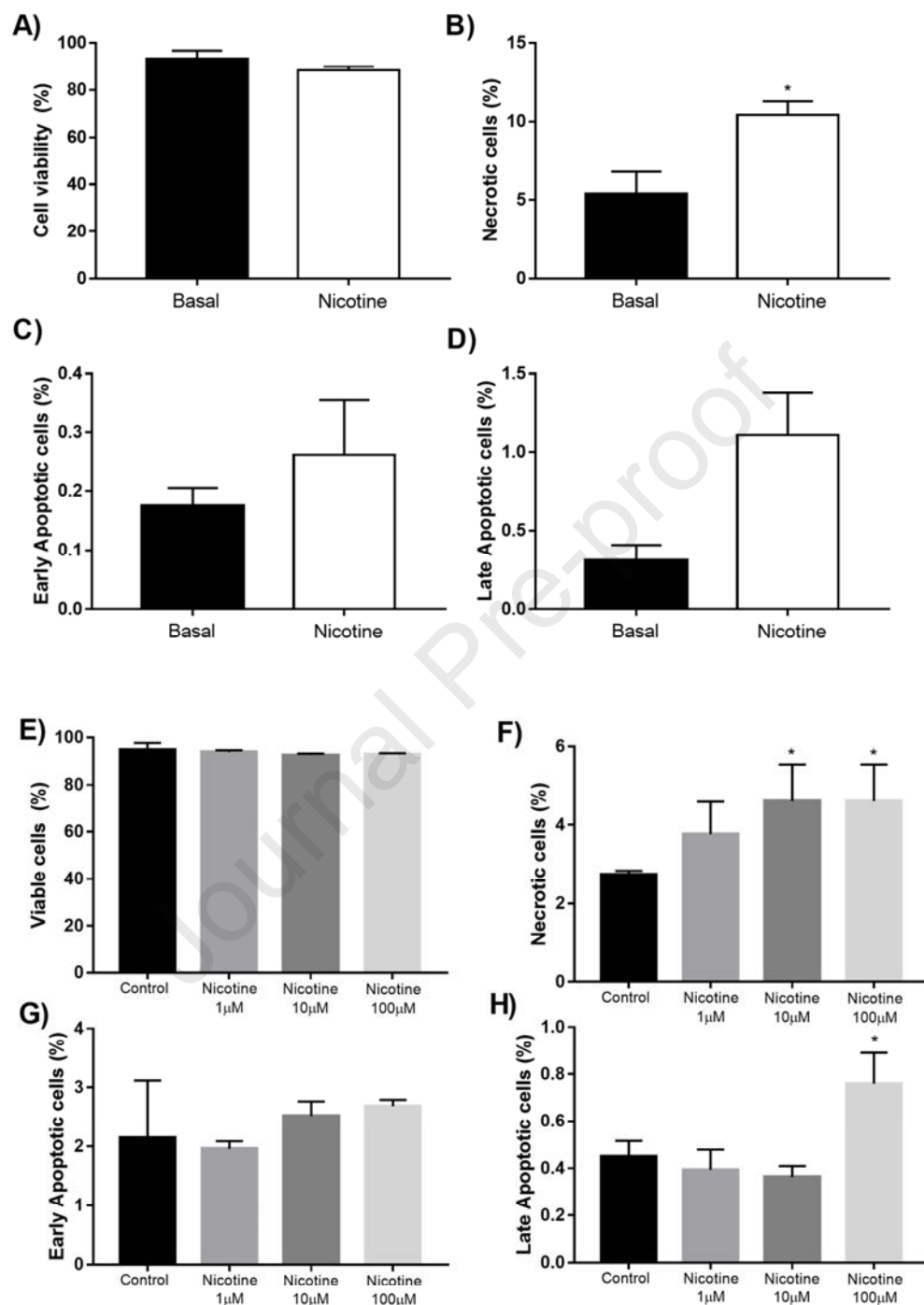


1022 **Supplementary Figure 3.**
1023

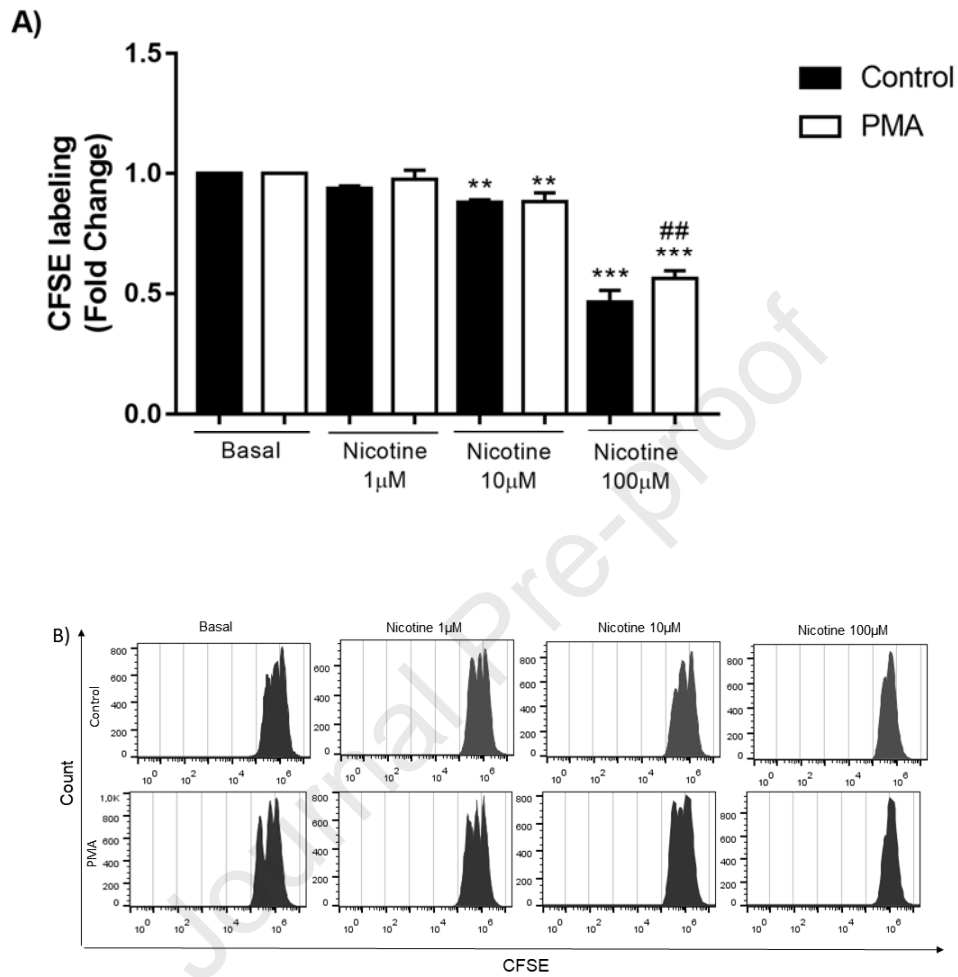


1024
1025
1026
1027
1028
1029
1030
1031
1032
1033
1034

1035 **Supplementary Figure 4.**
1036



Supplementary Figure 5.



Highlights

- CS exposure led to higher incidence of late-apoptosis and necrosis than HNBT;
- Only CS exposure caused DNA damage, oxidative stress and cytokines secretion by Jurkat cell;
- Only CS exposure caused significant *in vivo* and *in vitro* metallothioneins expression;
- CS, HNBT vapor or nicotine exposures impaired interleukin-2 secretion and Jurkat T cell proliferation;
- The toxicity caused by HNBT vapor exposure is related to nicotine harmful actions;

Declaration of interests

☒ The authors declare that they have no known competing financial interests or personal relationships that could have appeared to influence the work reported in this paper.

☐ The authors declare the following financial interests/personal relationships which may be considered as potential competing interests: